Int J Thermophys (2007) 28:2098–2110
DOI 10.1007/s10765-007-0244-5

Propagation of Uncertainty Due to Non-linearity in Radiation Thermometers

P. Saunders · D. R. White

Published online: 31 August 2007

Abstract The measurement of the non-linearity of radiation thermometers is important in the realization of ITS-90 above the silver point and in the calibration of primary or secondary radiation thermometers using multiple fixed points both above and below the silver point. A non-linearity function is usually derived, enabling correction of the measured signals. Uncertainties in this non-linearity function propagate to the uncertainty in the determination of an unknown temperature. Since the same non-linearity function is used both during calibration and in subsequent use of the thermometer, there is a high degree of correlation between the uncertainties in the corrected calibration signals and the corrected in-use signals. While these correlations obviously lead to zero uncertainty at the calibration points, it is difficult to determine the correlation coefficients for temperatures away from these points. This article sets out a mathematical framework, based on interpolation theory, for propagating the uncertainty due to non-linearity in which correlation is easily included. The method is illustrated for a thermometer realizing ITS-90 up to 3,000°C based on one fixed point (silver, gold, or copper), and also for alternative realization schemes based on two or more fixed points. The total non-linearity uncertainty for the multipoint schemes is considerably lower than for the ITS-90 method. The mathematical framework can also be applied to secondary calibrations below the silver point, where non-linearity is typically more problematic for the detectors used in this temperature range.

Keywords Non-linearity · Radiation thermometry · Uncertainty

P. Saunders (✉) · D. R. White
Measurement Standards Laboratory of New Zealand, Industrial Research Ltd.,
P.O. Box 31-310, Lower Hutt, New Zealand
e-mail: p.saunders@irl.cri.nz

1 Introduction

Above the freezing point of silver (961.78°C), ITS-90 is defined in terms of the spectral radiance of blackbodies and is realized using radiation thermometers. Temperatures are calculated from the ratio of the signal measured at the unknown temperature to that at either one of the silver, gold, or copper points, along with a determination of the relative spectral responsivity of the thermometer. Secondary realizations of ITS-90 below the silver point are also carried out, without measuring the spectral responsivity, by interpolating signals measured at multiple fixed points with a calibration equation. With the recent development of high-temperature fixed points based on metal–carbon [1] and metal-carbide–carbon eutectics [2], this interpolation scheme may, in the future, be adopted as a primary method above the silver point [3].

In all of these methods, it is important to characterize the non-linearity in the signal response of the thermometer in order for its reading to faithfully follow Planck's law. There are well-established techniques for determining a radiation thermometer's non-linearity that enable corrections to be applied to the measured signals [4–9]. Application of these corrections, however, results in a degree of uncertainty which impacts on the uncertainty in the measured temperature. This non-linearity uncertainty has been identified as one of the dominant components in the realization of ITS-90 [10].

Determining how uncertainties in the correction for non-linearity propagate to uncertainty in a measured temperature is complicated by the use of the same data to correct signals during both calibration and subsequent use of the thermometer (for ITS-90 realization, calibration here refers to the measurement of the signal at the reference fixed point). This practice introduces complicated correlations into the uncertainty analysis. Methods for dealing with this non-linearity uncertainty are considered in this article. For the sake of clarity, all other uncertainty components are assumed to be zero.

2 Calibration Schemes

The signal, $S(T)$, measured by a radiation thermometer at temperature T is given by the integral,

$$S(T) = \int_0^\infty R(\lambda) L_\mathrm{b}(T, \lambda) d\lambda, \tag{1}$$

where $R(\lambda)$ is the spectral responsivity of the thermometer (including all geometrical, optical, and electrical factors) and $L_\mathrm{b}(\lambda, T)$ is the spectral radiance of a blackbody at temperature T and wavelength λ, given by Planck's law. In order to simplify the uncertainty analysis, Eq. 1 will be modeled by the algebraic function,

$$S(T) = \frac{C}{\exp\left(\frac{c_2}{AT+B}\right) - 1}, \tag{2}$$

where c_2 is the second radiation constant and the parameters A, B, and C are all related to the thermometer's spectral responsivity [3]:

$$A = \lambda_0 \left(1 - 6r^2\right), \tag{2a}$$

$$B = \frac{c_2}{2} r^2, \tag{2b}$$

$$C = \frac{c_1}{\lambda_0^5} \left(1 + 15r^2\right) H. \tag{2c}$$

In these equations, λ_0 is the mean wavelength of the spectral responsivity; r is the relative bandwidth of the spectral responsivity, $r = \sigma/\lambda_0$, where σ is the standard deviation and is directly proportional to the full width at half maximum; $H = \int_0^\infty R(\lambda) d\lambda$ is the area under the spectral responsivity curve; and c_1 is the first radiation constant. Note that the determinations of both λ_0 and r require knowledge only of the relative, not absolute, spectral responsivity. Equation (2) is the Sakuma–Hattori equation [11,12], and its accuracy has been well established [13]. Equations (2a–2c) for its parameters are valid when $r \ll 1$, in which case Eq. 2 is in error by only a few millikelvin up to 3,000°C. This error is small compared to other uncertainty components, including that arising from non-linearity, and can be considered negligible. Furthermore, at the wavelengths of 650 and 900 nm, normally used to realize ITS-90, the Wien approximation to Eq. 2, namely, neglecting the -1 in the denominator, introduces negligible error up to 3,000°C.

While Eq. 2 has traditionally been used as an interpolation equation, with the parameters A, B, and C determined by curve fitting to at least three temperature-signal data points, it need not be restricted to this. The equation is equally valid for all methods of determining A, B, and C. Thus, the ITS-90 primary method of calculating temperature through signal ratios and integration of Eq. 1 may be recast directly into the application of Eq. 2 by first determining A and B using Eqs. 2a and 2b from a measurement of the relative spectral responsivity, and then determining C using Eq. 2 based on a measurement of $S(T_{\mathrm{ref}})$ at the reference fixed point. This single fixed-point method is referred to as an $n = 1$ calibration scheme. Similarly, $n = 2$ schemes are valid [14], whereby the bandwidth, σ, of the spectral responsivity, for example, is first estimated, then two fixed points are used to determine λ_0 and H, thereby allowing A, B, and C all to be determined. The well-known $n = 3$ interpolation scheme and $n > 3$ least-squares scheme allow Eq. 2 to be implemented without any knowledge of the spectral responsivity. Although not discussed in this article, Eq. 2 is also valid for an $n = 0$ thermodynamic determination of temperature in which λ_0, r, and H are measured directly.

Non-linearity affects each of the $n \geq 1$ schemes during measurement of each of the n fixed-point signals, as well as during subsequent measurement of the signal at the unknown temperature. Propagation of uncertainty in the non-linearity corrections

of these signals for the cases $n = 1$, $n = 2$, $n = 3$, and $n > 3$ will be analyzed below. First, a non-linearity function is defined.

3 The Non-linearity Function

It is assumed that non-linearity in a radiation thermometer's signal is largely caused by non-linearity in the detector's response, with minimal contribution from the amplifier or changes in gain. The non-linearity in the signal, S', measured by a radiation thermometer can, thus, be corrected by determining a continuous non-linearity function $\eta(S')$, such that the linearized signal, S, is simply given by

$$S = \eta(S') \times S'. \tag{3}$$

There are two classes of methods used to determine the non-linearity function, "dual aperture" (DA) [4,5] and "superposition" (SP) [6,7,9] methods, both of which sample the non-linearity at a number, m, of discrete measured signal values spanning the range of signals for which the thermometer is to be used. The continuous function $\eta(S')$ can then be characterized by interpolating (or least-squares fitting) these points, η_j for j=1 to m, with an assumed functional form.

3.1 Dual Aperture Methods

In the DA methods, signals S'_A and S'_B from two sources are measured individually and then compared to the signal S'_{A+B}, measured by optically combining the two sources. The measured non-linearity for this series of measurements is

$$\eta'_{A+B} = \frac{S'_A + S'_B}{S'_{A+B}}. \tag{4}$$

Note that this measured non-linearity (denoted η') is not the true non-linearity because the signals S'_A and S'_B are themselves subject to non-linearity. The cumulative nature of the DA methods must be unraveled to determine the true non-linearity values η_j.

To simplify the analysis, it is assumed that the two individual signals are arranged to be equal ($S'_A = S'_B \equiv S'_0$ and $S'_{A+B} \equiv S'_1$) so that this DA method becomes a flux-doubling method. The value of S'_0 is typically chosen to be close to the lowest operating signal, and is successively doubled up to the highest operating signal. The measured non-linearity at the first doubling is

$$\begin{aligned} \eta'_1 &= \frac{S'_0 + S'_0}{S'_1} \\ &= \frac{2S_0}{S'_1 \eta_0}, \end{aligned}$$

where S_0 is the linearized signal corresponding to S'_0 and η_0 is its true non-linearity value, which is unknown. Flux-doubling proceeds by doubling the signal S'_1 to give S'_2, and so on. In general, after k doublings, the measured non-linearity is

$$\eta'_k = \frac{2^k S_0}{S'_k \eta_0 \prod_{j=1}^{k-1} \eta'_j}. \tag{5}$$

Recognizing that $2^k S_0 = S_k$, it can be seen that Eq. 5 gives the true non-linearity for the measured signal S'_k as

$$\eta_k = \eta_0 \prod_{j=1}^{k} \eta'_j. \tag{6}$$

Thus, each non-linearity value simply accumulates geometrically from the previous value. The problem of Eq. 6 containing the unknown non-linearity, η_0, will be dealt with below.

3.2 Superposition Methods

The SP methods are combinatorial methods in which a number of different flux levels are generated using a series of filters [6,7,9]. The signal measurements are combined with a model of the non-linearity in such a way that a series of equations can be set up to solve for the unknown flux levels, the filter transmissions, and the parameters of the non-linearity model.

The non-linearity value at each signal level is then given by

$$\eta_j = K \frac{\phi_j}{S'_j}, \tag{7}$$

where ϕ_j is the solved value of the flux corresponding to the measured signal S'_j and K is an unknown proportionality factor between flux and signal imposed by the design of the radiation thermometer. Thus, as for the dual aperture methods, the non-linearity function given by Eq. 7 can only be determined, without additional information, up to a multiplicative factor.

3.3 Radiation Thermometry Measurements on ITS-90

Accurate thermodynamic measurements require the determination of η_0 or K in Eq. 6 and Eq. 7, respectively. However, for measurements on ITS-90, this is not the case. The $n = 1$ primary and $n > 1$ secondary determinations of ITS-90 are not affected by lack of knowledge of η_0 or K because these factors are absorbed by the C coefficient in Eq. 2. Thus, for all purposes other than $n = 0$ thermodynamic measurements, the

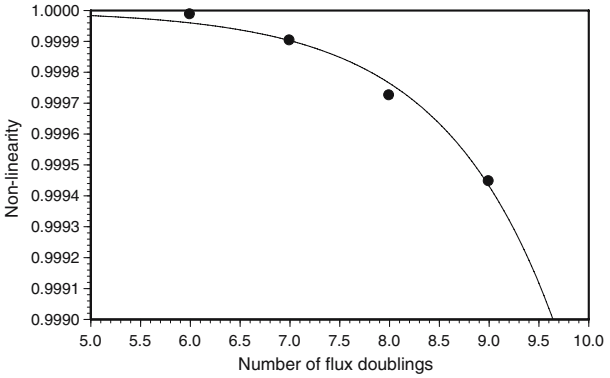

Fig. 1 Non-linearity data (circles) generated with Eq. 6 from measured signals using the flux doubling technique, and the fitted non-linearity function given by Eq. 9 (line). Fitted parameters are $a = -2 \times 10^{-7}$ and $c = 1.27$

non-linearity functions of Eqs. 6 and 7 can be redefined by setting $\eta_0 = K = 1$. This will be implicit in the remainder of this article.

3.4 Functional Form

The discrete non-linearity data points, η_j, obtained from either Eq. 6 or 7 can be fitted by a functional form to allow non-linearity corrections to be made for any arbitrary measured signal. A relatively simple form suggested for silicon detectors [5] is

$$\eta(S') = 1 - \left(a + bS'^{c}\right), \tag{8}$$

where a, b, and c are adjustable parameters. If a flux-doubling method is used, then an equivalent form of Eq. 8 is

$$\eta(x) = 1 - a\left(1 - 2^{cx}\right), \tag{9}$$

where $x = \log_2\left(S'/S'_0\right)$ is the effective number of flux doublings from the initial signal S'_0. Equations (8) and (9) are directly related through $b = -a/S'^{c}_0$.

Experimental data for an InGaAs detector also fit Eq. 9, as illustrated in Fig. 1. Here, the initial signal S'_0 corresponds to the zinc point, and the values of the parameters are $a = -2 \times 10^{-7}$ and $c = 1.27$.

4 Propagation of Uncertainty

The Sakuma–Hattori equation (2) can, in principle, be written explicitly in the form,

$$S = S(T; \lambda_0, r; T_1, T_2, \ldots, T_n, S_1, S_2, \ldots, S_n), \tag{10}$$

where $(T_1, S_1), (T_2, S_2), \ldots, (T_n, S_n)$ are the n calibration points and T is the unknown temperature (for the $n = 2$ scheme, λ_0 would not appear in the parameter list, and for $n \geq 3$, neither λ_0 nor r would appear). The propagation-of-error equation is obtained by differentiating Eq. 10 with respect to all of the measured variables. However, as mentioned in Sect. 1, in this article all errors other than those due to corrections for non-linearity are assumed to be zero, so the propagation-of-error equation is

$$\mathrm{d}S = \frac{\partial S}{\partial T}\mathrm{d}T + \sum_{i=1}^{n} \frac{\partial S}{\partial S_i}\mathrm{d}S_i, \tag{11}$$

where the $\mathrm{d}S_i$ values are the errors in the signals at the calibration points after correcting for non-linearity, and $\mathrm{d}T$ is the error in the unknown temperature. The $\partial S/\partial S_i$ factors are sensitivity coefficients, whose forms depend on the value of n. The factor $\partial S/\partial T$ is the derivative of the Sakuma–Hattori equation, which under the Wien approximation is

$$\frac{\partial S}{\partial T} = \frac{c_2}{\lambda_T T^2} S, \tag{12}$$

where λ_T is the limiting effective wavelength evaluated at T, given by [15]

$$\lambda_T = A\left(1 + \frac{B}{AT}\right)^2. \tag{13}$$

The quantity of most interest in Eq. 11 is $\mathrm{d}T$, the error in the measured temperature, which by rearrangement is given by

$$\mathrm{d}T = \left(\mathrm{d}S - \sum_{i=1}^{n} \frac{\partial S}{\partial S_i}\mathrm{d}S_i\right) \Bigg/ \left(\frac{\partial S}{\partial T}\right) = \frac{\lambda_T T^2}{c_2}\left(\frac{\mathrm{d}S}{S} - \sum_{i=1}^{n} \frac{\partial S}{\partial S_i}\frac{S_i}{S}\frac{\mathrm{d}S_i}{S_i}\right). \tag{14}$$

We can now recognize the first term on the right-hand side of the first equality as the signal error when the thermometer is used (after calibration) and the other n terms as the errors arising from the calibration signals at the fixed points. The second equality expresses the signal errors as relative values. These are simply related to the error in the non-linearity function of Eq. 3 by

$$\frac{\mathrm{d}S}{S} \approx \frac{\mathrm{d}S}{S'} = \mathrm{d}\eta(S'). \tag{15}$$

Thus, the error in Eq. 14 can be written directly in terms of the errors in the non-linearity function. The sensitivity coefficients $\partial S/\partial S_i$ for each value of n are required to completely specify Eq. 14. These are given below.

4.1 The $n = 1$ Scheme

Reference [16] gives general methods for calculating sensitivity coefficients for interpolation and least-squares fitting. However, for the $n = 1$ ITS-90 scheme, it is easier to simply solve for the C coefficient in the Sakuma–Hattori equation (2) based on the signal measurement, $S_1 = S_{\mathrm{ref}}$, at the reference fixed point and then differentiate the resulting equation:

$$\frac{\partial S}{\partial S_1} = \frac{S}{S_1}. \tag{16}$$

Substituting this into Eq. 14 with $n = 1$, and using Eq. 15, gives

$$\mathrm{d}T = \frac{\lambda_T T^2}{c_2}\left(\frac{\mathrm{d}S}{S} - \frac{\mathrm{d}S_1}{S_1}\right) = \frac{\lambda_T T^2}{c_2}\left[\mathrm{d}\eta(S') - \mathrm{d}\eta(S'_1)\right]. \tag{17}$$

Note that $\mathrm{d}T = 0$ when $S' = S'_1$. Of course, in general, the errors $\mathrm{d}\eta(S')$ in the non-linearity function are unknown, so Eq. 17 must be turned into an uncertainty equation. Following the GUM [17], this is

$$u^2(T) = \left(\frac{\lambda_T T^2}{c_2}\right)^2 \left[u^2\left(\eta(S')\right) + u^2\left(\eta(S'_1)\right) - 2r(S', S'_1)u\left(\eta(S')\right)u\left(\eta(S'_1)\right)\right], \tag{18}$$

where $r(S', S'_1)$ is the correlation coefficient between the uncertainties in the non-linearity function evaluated at S' and S'_1. While this correlation coefficient is clearly equal to 1 when $S' = S'_1$, so that $u(T_1) = 0$ at the reference fixed point, as mentioned above, at other temperatures it is generally not easy to determine the value of r. This becomes even more difficult when $n > 1$. Note that if the non-linearity function has been determined using a dual aperture method, and if the initial signal corresponds to the reference fixed point ($S'_0 = S'_1$), then the uncertainty component $u\left(\eta(S'_1)\right)$ is zero for a non-linearity function given by Eq. 9 since $\eta(S'_0) = 1$ by definition. This simplifies Eq. 18 and eliminates the correlation coefficient problem. This problem re-emerges, however, for $n > 1$.

4.2 The $n = 2$ and $n = 3$ Schemes

For $n = 2$ and $n = 3$, the interpolation theory methods of Refs. [16] and [18] give

$$\frac{\partial S}{\partial S_i} = \frac{S}{S_i}\frac{\lambda_{T_i}}{\lambda_T}\left(\frac{T_i}{T}\right)^{n-1} L_i^{(n-1)}(T), \tag{19}$$

where $L_i^{(n)}(T)$ are Lagrange polynomials in T of order n. Thus

$$L_1^{(1)}(T) = \frac{T - T_2}{T_1 - T_2},\ L_2^{(1)}(T) = \frac{T - T_1}{T_2 - T_1}, \tag{20}$$

and

$$\begin{aligned} L_1^{(2)}(T) &= \frac{(T - T_2)(T - T_3)}{(T_1 - T_2)(T_1 - T_3)},\ L_2^{(2)}(T) = \frac{(T - T_1)(T - T_3)}{(T_2 - T_1)(T_2 - T_3)}, \\ L_3^{(2)}(T) &= \frac{(T - T_1)(T - T_2)}{(T_3 - T_1)(T_3 - T_2)}. \end{aligned} \tag{21}$$

The Lagrange polynomials have the property that $L_i(T_j) = \delta_{ij}$ for all orders. Note that the Wien approximation to the Sakuma–Hattori equation has been used in deriving Eq. 19. The full Planck version would require replacing the Lagrange polynomials with more complicated functions [19], but for thermometers operating at 650 or 900 nm up to 3,000°C, the resulting uncertainty is not significantly different. The propagation-of-error equation (14) becomes

$$\mathrm{d}T = \frac{\lambda_T T^2}{c_2}\mathrm{d}\eta(S') - \sum_{i=1}^{n} \frac{\lambda_{T_i}}{c_2} T_i^{n-1} T^{3-n} L_i^{(n-1)}(T)\mathrm{d}\eta(S_i'). \tag{22}$$

As for $n = 1$, $\mathrm{d}T = 0$ at all the calibration points, since $L_i(T_j) = \delta_{ij}$. The propagation-of-uncertainty equation corresponding to Eq. 22 is formed in a similar way to Eq. 18. For $n = 2$, this contains three quadrature terms and three correlation terms, while for $n = 3$ there are four quadrature terms and six correlation terms. Writing out the propagation-of-uncertainty equation in full, it is easily seen that at each of the calibration points the total uncertainty due to the non-linearity is zero. However, away from the calibration points, there are again unknown correlation coefficients.

4.3 The $n > 3$ Scheme

When $n > 3$, solving for the A, B, and C parameters of the Sakuma–Hattori (2) requires the use of least-squares methods. Reference 16 again provides a method for calculating the $\partial S/\partial S_i$ sensitivity coefficients, but they are too complex to write down in a compact algebraic form and are more conveniently calculated numerically.

4.4 Elimination of Unknown Correlations

The problem of unknown correlation coefficients occurring in the propagation-of-uncertainty equations discussed above arises because of the three-step mathematical process adopted: first the discrete non-linearity data points are measured; then a continuous non-linearity function is derived by curve fitting; and finally the uncertainties in this fitted curve are propagated through the Sakuma-Hattori equation to the unknown

temperature. The correlations are introduced in going from the second to third step. We can eliminate these correlations by bypassing this step and propagating the uncertainties in the discrete non-linearity data directly to the Sakuma–Hattori equation.

In order to do this, we need to express the error in the non-linearity function, $\mathrm{d}\eta(S')$, directly in terms of the errors in the discrete non-linearity measurements, $\mathrm{d}\eta_j$. Using interpolation theory [16,20] again, this can be written as

$$\mathrm{d}\eta(S') = \sum_{j=1}^{m} \mathrm{d}\eta_j \, f_j(S'), \tag{23}$$

where $f_j(S')$ are the required sensitivity coefficients. These are relatively easy to calculate, but for most realistic non-linearity functions their form is somewhat complex to write down. Substituting Eq. 23 into Eq. 14 gives

$$\begin{aligned} \mathrm{d}T &= \frac{\lambda_T T^2}{c_2} \left(\sum_{j=1}^{m} \mathrm{d}\eta_j \, f_j(S') - \sum_{i=1}^{n} \frac{\partial S}{\partial S_i} \frac{S_i}{S} \sum_{j=1}^{m} \mathrm{d}\eta_j \, f_j(S_i') \right) \\ &= \sum_{j=1}^{m} \mathrm{d}\eta_j \left[\frac{\lambda_T T^2}{c_2} f_j(S') - \sum_{i=1}^{n} \frac{\lambda_T T^2}{c_2} \frac{\partial S}{\partial S_i} \frac{S_i}{S} f_j(S_i') \right]. \end{aligned} \tag{24}$$

The advantage of Eq. 24 is that the entire factor in square brackets is the sensitivity coefficient, c_j, for the error in the measured non-linearity value, $\mathrm{d}\eta_j$, when propagated directly to the unknown temperature. The propagation of the uncertainty equation will only contain correlation terms between the discrete non-linearity points, $r(\eta_j, \eta_k)$, for which the correlation coefficients are easily determined. Following the GUM [17],

$$u^2(T) = \sum_{j=1}^{m} \sum_{k=1}^{m} c_j c_k r(\eta_j, \eta_k) u(\eta_j) u(\eta_k), \tag{25}$$

where

$$c_j = \left[\frac{\lambda_T T^2}{c_2} f_j(S') - \sum_{i=1}^{n} \frac{\lambda_T T^2}{c_2} \frac{\partial S}{\partial S_i} \frac{S_i}{S} f_j(S_i') \right]. \tag{26}$$

For the $n = 1$, 2, and 3 schemes, the sensitivity coefficients are explicitly

$$n = 1: \; c_j = \frac{\lambda_T T^2}{c_2} \left[f_j(S') - f_j(S_1') \right], \tag{27}$$

$$n = 2: \; c_j = \frac{T}{c_2} \left[\lambda_T T \, f_j(S') - \sum_{i=1}^{2} \lambda_{T_i} T_i L_i^{(1)}(T) f_j(S_i') \right], \tag{28}$$

$$n = 3: \; c_j = \frac{1}{c_2}\left[\lambda_T T^2 f_j(S') - \sum_{i=1}^{3} \lambda_{T_i} T_i^2 L_i^{(2)}(T) f_j(S_i')\right]. \tag{29}$$

In all cases, the factor in square brackets in each sensitivity coefficient is the interpolation error resulting from an $(n-1)$th polynomial interpolation (Lagrange interpolation) through the function defined by the term before the minus sign [18]. Each sensitivity coefficient c_j, therefore, has n zeros at the fixed-point temperatures. For example, for $n = 3$, $\sum_{i=1}^{3} \lambda_{T_i} T_i^2 L_i^{(2)}(T) f_j(S_i')$ is a quadratic interpolation of the function $\lambda_T T^2 f_j(S')$, so the difference has zeros at T_1, T_2, and T_3. This is exactly what was expected from Eq. 22 when the correlations were considered, but Eqs. 25–29 give all the additional information about the propagated uncertainty between the fixed points. When $n > 3$, there are still three zeros in the propagated uncertainty, since there are three free parameters in the Sakuma–Hattori equation, which occur at three points within the fitted temperature range, but not necessarily at the fixed-point temperatures.

5 Example

To illustrate the use of Eqs. 25–29, this section considers a narrowband 650 nm thermometer whose non-linearity function has been measured using the flux-doubling method with S_0' corresponding to the copper point. The non-linearity uncertainty is propagated over the temperature range from 1,000 to 3,000°C for each of the $n = 1, 2,$ and 3 calibration schemes. It is assumed that the non-linearity function follows Eq. 8 with the fitted value of c equal to 0.5 (note, the values of a and b are unnecessary to propagate the uncertainty). This value of c is consistent with the experimental data in [5] for a silicon photodiode.

It is also assumed that the uncertainty in each measured non-linearity point is $u(\eta_j') = 3 \times 10^{-4}$ for j =1–14 ($m = 14$ flux doublings are required to reach 3,000°C from the copper point at 650 nm), corresponding to the "normal" accuracy value given in [10]. The uncertainties in the true non-linearity points calculated from the measured points using Eq. 6 are $u(\eta_1) = 3 \times 10^{-4}$ and

$$u(\eta_j) = \left[u^2(\eta_{j-1}) + u^2(\eta_j')\right]^{1/2} \quad \text{for } j = 2 \text{ to } 14. \tag{30}$$

From Eq. 6 and Ref. 17, the correlation coefficients between each of these uncertainties is

$$r(\eta_j, \eta_k) \approx \begin{cases} \sqrt{j/k} \text{ for } j \le k \\ \sqrt{k/j} \text{ for } j > k. \end{cases} \tag{31}$$

Figure 2 shows each of the 14 $f_j(S')$ functions for Eq. 8 that appear in the sensitivity coefficients of Eq. 26, where the horizontal axis has been converted to the equivalent temperature. Each curve is zero at the temperature corresponding to S_0'. Figure 3 gives the full uncertainty, given by the square root of Eq. 25, for each of the calibration

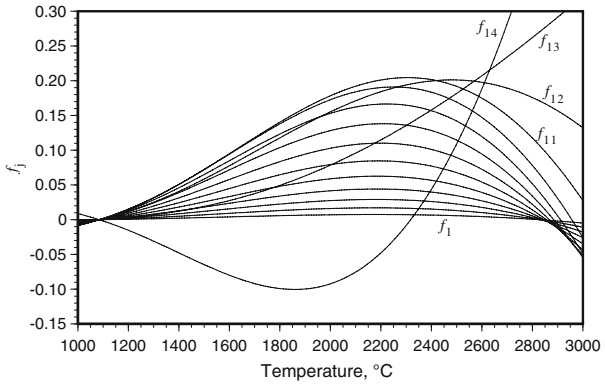

Fig. 2 The 14 $f_j(S')$ functions for Eq. 8. The horizontal axis has been converted from detected signal to equivalent temperature

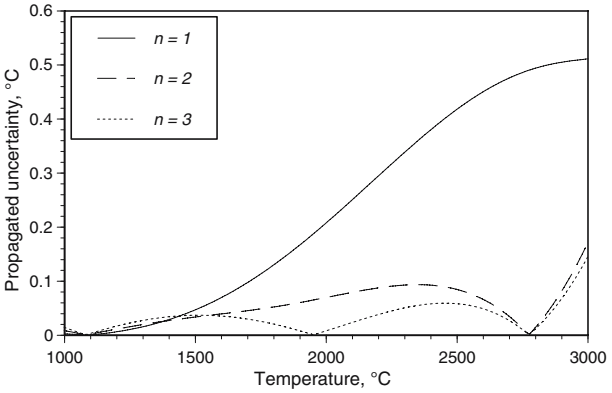

Fig. 3 Propagated uncertainty due to non-linearity for the $n = 1$, 2, and 3 calibration schemes. The calibration temperatures are: $T_1 = 1084.62°C$ for $n = 1$; $T_1 = 1084.62°\text{C}$, $T_2 = 2776°\text{C}$ for $n = 2$; and $T_1 = 1084.62°\text{C}$, $T_2 = 1953°\text{C}$, $T_3 = 2776°\text{C}$ for $n = 3$

schemes. The calibration temperatures for each scheme are evident from where the curves go to zero. The shapes of these curves depend somewhat on the assumed form of the non-linearity function and the number of flux-doublings involved. However, in general, the $n = 2$ and $n = 3$ secondary schemes show a clear advantage over the primary $n = 1$ scheme in minimizing the uncertainty due to non-linearity, since the multiple fixed points tend to constrain the uncertainties within the interpolation region.

6 Conclusion

A mathematical formalism has been presented that allows uncertainties in the corrections for signal non-linearity to be propagated directly to the measured temperature. Some recently published results from interpolation theory have formed an essential part of this formalism, allowing correlations between calibration uncertainties

and in-use uncertainties to be included in a simplified manner. Modeling of the signal response of a radiation thermometer with the Sakuma–Hattori equation has allowed analytic expressions to be derived for the uncertainties for each of the various calibration schemes. This enables easy comparison among the schemes and possible optimization of uncertainty through judicious choice of thermometer and calibration parameters. The formalism presented here can also be extended to include all other uncertainty components in the present and future implementations of the radiation thermometry part of the International Temperature Scale.

References

1. Y. Yamada, N. Sasajima, F. Sakuma, A. Ono, in *Proc. TEMPMEKO 2001, 8th International Symposium on Temperature and Thermal Measurements in Industry and Science*, ed. by. B. Fellmuth, J. Seidel, G. Scholz (VDE Verlag GmbH, Berlin, 2002), pp. 19–26
2. N. Sasajima, Y. Yamada, F. Sakuma, in *Temperature: Its Measurement and Control in Science and Industry*, vol. 7, ed. by D. C. Ripple (AIP, Melville, New York, 2003), pp. 279–284
3. P. Saunders, D.R. White, Metrologia **40**, 195 (2003)
4. K.D. Mielenz, K.L. Eckerle, Appl. Optics **11,** 2294 (1972)
5. H.J. Jung, Metrologia **15**, 173 (1979)
6. L. Coslovi, F. Righini, Appl. Optics **19**, 3200 (1980)
7. R.D. Saunders, J.B. Shumaker, Appl. Optics **23**, 3504 (1984)
8. J.F. Clare, Meas. Sci. Technol. **13**, N38 (2002)
9. H.W. Yoon, J.J. Butler, T.C. Larason, G.P. Eppeldauer, Metrologia **40**, S154 (2003)
10. J. Fischer, M. Battuello, M. Sadli, M. Ballico, S.N. Park, P. Saunders, Y. Zundong, B.C. Johnson, E. van der Ham, F. Sakuma, G. Machin, N. Fox, W. Li, S. Ugur, M. Matveyev, in *Temperature: Its Measurement and Control in Science and Industry*, vol. 7, ed. by D.C. Ripple (AIP, Melville, New York, 2003), pp. 631–638
11. F. Sakuma, S. Hattori, in *Temperature: Its Measurement and Control in Science and Industry*, vol. 5, ed. by J.F. Schooley (AIP, New York, 1982), pp. 421–427
12. F. Sakuma, M. Kobayashi, in *Proc. TEMPMEKO '96, Sixth International Symposium on Temperature and Thermal Measurements in Industry and Science*, ed. by P. Marcarino (Levrotto and Bella, Torino, 1997), pp. 305–310
13. P. Saunders, D.R. White, Metrologia **41**, 41 (2004)
14. P. Saunders, P. Bloembergen, D.R. White, *Proc. TEMPMEKO 2004, 9*th *International Symposium on Temperature and Thermal Measurements in Industry and Science*, ed. by D. Zvizdic (LPM FSB, Zagreb, 2005), pp. 1149–1154
15. P. Saunders, Metrologia **34**, 201 (1997)
16. P. Saunders, Metrologia **40**, 93 (2003)
17. Guide to the Expression of Uncertainty in Measurement (International Organization for Standardization, Geneva, 1993)
18. D.R. White, P. Saunders, Metrologia **37**, 285 (2000)
19. J. Fischer, P. Saunders, M. Sadli, M. Battuello, C.W. Park, Y. Zundong, H. Yoon, W. Li, E. van der Ham, F. Sakuma, Y. Yamada, M. Ballico, G. Machin, N. Fox, J. Hollandt, M. Matveyev, P. Bloembergen, S. Ugur, CCT working document (in preparation)
20. D.R. White, P. Saunders, Meas. Sci. Technol. **18**, 2157 (2007)